SCHOENFLIES, A. (1923). *Theorie der Kristallstruktur.* Berlin: Borntraeger.

SEIFERT, K. F. (1963). *Acta Cryst.* **16** (Supplement), A-16, Paper 2.17.

SMITH, G. S. & ALEXANDER, L. E. (1963). *Acta Cryst.* **16**, 462–471.

Strukturbericht (1931). Vol. 1. Leipzig: Akademische Verlagsges.

UNGEMACH, H. (1935). *Z. Kristallogr.* A**91**, 97–113.

VAN DER BIEST, O. & THOMAS, G. (1977). *Acta Cryst.* A**33**, 618–621.

VRIES, A. DE (1958). *Nature (London)*, **181**, 1193.

WEI, P. (1935). *Z. Kristallogr.* **92**, 355–362.

WOOSTER, W. A. (1953). *Rep. Prog. Phys.* **16**, 62–82.

WYCKOFF, R. W. G. (1922). *The Analytical Expression of the Results of the Theory of Space Groups.* 1st ed. Washington, D.C.: Carnegie Institution of Washington (Publication No. 318). (2nd ed., 1930.)

WYCKOFF, R. W. G. (1931). *The Structure of Crystals.* 2nd ed. New York: Chemical Catalog Co. (1st. ed., 1924). See p. 242.

WYCKOFF, R. W. G. (1948). *Crystal Structures.* Vol. I. New York: Interscience. (2nd ed., 1963, see p. 312.)

YOUNG, R. A. & POST, B. (1962). *Acta Cryst.* **15**, 337–346.

ZACHARIASEN, W. H. (1965). *Acta Cryst.* **18**, 715–717.

ZACHARIASEN, W. H. & PLETTINGER, H. A. (1965). *Acta Cryst.* **18**, 710–714.

X-ray Study of the Atomic Charge Densities in MgO, CaO, SrO and BaO*

BY G. VIDAL-VALAT AND J. P. VIDAL

Groupe de Dynamique des Phases Condensées, Université des Sciences et Techniques du Languedoc, 34060 Montpellier CEDEX, France

AND K. KURKI-SUONIO

Department of Physics, University of Helsinki, SF-00170, Helsinki, Finland

Accurate X-ray structure factors of CaO, SrO and BaO were measured at 293 K from single crystals and analysed together with the data of Sanger [*Acta Cryst.* (1969), A**25**, 694–702] on MgO. The oxygen ion is seen to suffer an average compression and a fourth-order cubic harmonic type deformation, as compared to the atomic superposition model, yielding a lower average charge density in the surrounding region and a charge transfer from [111] to the [100] direction. These features strengthen with increasing atomic number of the cation. Mg and Ca show a weak broadening. About nine electrons are localized around the oxygen position. The tenth electron of O^{2-} is more widely distributed. The electron counts of the cation correspond most closely to Mg^+, Ca^{2+}, Sr^{2+} and Ba^{2+}. The results confirm the dominance of ionic character and increase of ionicity with increasing atomic number of the cation.

Introduction

By their chemical nature, the alkaline earth oxides should lie between the covalent III–V compounds and the alkali halides with ionic character. Experimental study of their electronic structure is therefore expected to yield information on the bonding mechanism in cases where neither of these simple models works well.

This paper refers to the series MgO, CaO, SrO and BaO with NaCl structure. General chemical and dielectric considerations (Phillips, 1970) indicate strong dominance of ionic character comparable to the alkali halides, increasing from MgO to BaO. The oxides show, however, slightly more covalent character than the corresponding fluorides with same core configuration (Son & Bartels, 1972).

Theoretical consideration of the bonding in these crystals meets difficulties since the doubly ionized oxygen is not stable in the free state, the stabilization resulting from its bonding into the crystal lattice. Furthermore, theoretical models in lattice dynamics seem not to give a satisfactory explanation of spectroscopic results, especially in the case of SrO and BaO (Galtier, 1973; Montaner, 1974; Rieder, Weinstein, Cardona & Bilz, 1973).

The electronic state of the oxygen in MgO has been subject to several theoretical calculations (Yamashita & Kojima, 1952; Watson, 1958; Suzuki, 1960; Tokonami, 1965; Yamashita & Asano, 1970) and to

several experimental studies (Togawa, 1965; Burley, 1965; Raccah & Arnott, 1967; Sanger, 1969) leading to different conclusions. The survey by Dawson (1969) noted the concordance between Togawa's and Burley's results that gave the best fit with the O^{2-} form factor obtained by a combination of Watson's (+2 well) and Yamashita's wave functions. Sanger's measurements on a neutron-irradiated MgO single crystal showed the best fit with a combination of Mg^{2+} and O^{2-} Watson (+2 well) form factors. Togawa, Inkinen & Manninen (1971) and Weiss (1970) concluded from their Compton profile measurements that the crystalline-field wave functions of Yamashita and of Yamashita & Asano described the outer electrons of O^{2-} better than the Watson model. These conclusions are, however, uncertain. If mutual orthogonality is imposed on the theoretical wave functions of neighbouring atoms, the calculated momentum distribution deviates significantly from the observed results for all of these atomic models (Paakkari, 1975).

There has been no comparable activity on the other three crystals. This work reports the first accurate measurements of X-ray structure factors of CaO, SrO and BaO and the subsequent charge-density analysis. The bonding nature and the effect of the bonding on the constituent atoms are studied. Particular attention is paid to possible observable systematics of O^{2-}.

For the present purpose, direct charge-density analysis (Vahvaselkä & Kurki-Suonio, 1975) is well suited. Analysis based merely on comparison of observed and theoretical structure factors might easily lead to erroneous conclusions on the state of atoms in the crystal (Kurki-Suonio & Salmo, 1971). For MgO, the data of Sanger (1969) were reanalysed in a similar manner.

Experimental

CaO, SrO and BaO single crystals of highest purities provided by Spicer Ltd (England) were grown by arc fusion under inert atmosphere, then quenched by a rapid cooling down to room temperature to produce a high degree of mosaicity. Because of high hygroscopy, the specimens were cleaved and cut from large crystals under paraffin oil. For the diffraction measurements the CaO and SrO crystals were coated with plastic, BaO

was sucked into a standard sealed Lindemann capillary tube. The protection efficiency was checked after one to six months of storage and was found safe. The plastic for the capillary was chosen after careful X-ray scattering studies of several materials. The scattering from the sample holder used was checked so that it gave no disturbing effect on the measurement.

Table 1 gives the crystallographic data of the crystals used.

Relative intensities were collected at 293 K in a whole octant on an automatic three-circle Enraf–Nonius CAD-3 using Mo $K\alpha$ radiation. The beam was reflected from a graphite monochromator, the polarization ratio of which was estimated as 0·95. The diffracted radiation was measured in the $\theta/2\theta$ scan mode at a scanning speed of $1'$ s^{-1}. The angular height and width of the detector window were $2°$ $12'$ and $58'$ respectively. To minimize the effect of fluorescent radiation (particularly from Sr) a pulse-height discriminator was used and a very narrow analyser window was chosen to distinguish between the characteristic radiations from neighbouring elements. The diffractometer performances (Denne, 1972) were tested. The combined estimated standard deviations for the stability of the X-ray source and the counting chain were found to be less than 0·5%. The errors in the uniformity of the active area and the beam homogeneity were estimated as 1% and 0·6% respectively.

The overall dead time of the counting circuit was 4 μs. At the maximum counting rate (2000 c.p.s.) occurring in the measurements this corresponds to a dead-time correction less than 1%.

Multiple scattering was eliminated by independent setting of crystallographic and diffractometer axes.

Lorentz–polarization, absorption (method of Busing & Levy, 1957) and anomalous-dispersion corrections were applied on intensities.

The data were corrected for thermal diffuse scattering with the isotropic approximation of Cooper & Rouse (1968) for first-order scattering and the elastic constants measured by Son & Bartels (1972) and Bartels & Vetter (1973).

The large number of lattice defects produced in the preparation made the extinction small. To check its order of magnitude the correction of Coppens & Hamilton (1970) was applied. The maximum effect of

Table 1. *Crystal data*

	MgO (Sanger, 1969)	CaO	SrO	BaO
Crystal volume (mm³)	0·12 × 0·12 × 0·12	0·33 × 0·24 × 0·36	0·15 × 0·15 × 0·22	0·19 × 0·38 × 0·32
Cell parameter (Å)	4·2147 (2)	4·819 (1)	5·176 (3)	5·539 (3)
Linear absorption coefficient (cm⁻¹) for Mo $K\alpha$ (Cromer & Liberman, 1970)		44·57	379·18	214·80

1–2% was found in the first reflections. This can be considered negligible, particularly since the model on which the correction is based does not correspond well to the type of sample used. Hence, no extinction correction is included in the data and in the numerical results given. A complete parallel analysis with the extinction-corrected data was, however, performed, but it did not show any significantly different results, thus giving a qualitative justification of this omission.

The octant measured was chosen to take into account a crystalline chemical inhomogeneity (Mil-ledge, 1969) mainly created by the growth method (Chen & Abraham, 1972). Equivalent reflections differing in integrated intensity by no more than 2 to 2·5% from the average were accepted. Others (up to 7 to 18% according to the compound) were discarded. The θ,χ,φ values of the excluded reflections were seen to belong to the same part of the crystal, depending on the specimen. The observed structure factor of a reflection was taken to be the mean of the remaining symmetry-related reflections.

The cell parameters (Table 1) were determined by least-squares calculations.

Preliminary treatment of data

The first phase of the analysis consisted of a deter-mination of the scale factor and the isotropic Debye–Waller factors B_+ and B_- for the cation and the oxygen respectively. For the cations the theoretical atomic factors of *International Tables for X-ray Crystallog-raphy* (1974) were used, while for the oxygen those of Sanger (1969) based on the +2-well wave functions of Watson (1958) for O^{2-} were adopted. The refinement was done with the iterative Fourier method of Vah-vaselkä & Kurki-Suonio (1975). In this procedure the dispersion corrections were made on the experimental structure factors using the $\Delta f'$ and $\Delta f''$ values of Cromer & Liberman (1970). The B values obtained in this way minimize the termination effects and are therefore preferable in analysis of atomic charge distributions.

The calculation was repeated with different cut-offs from 0·6 to 1·1 Å^{-1} in sin θ/λ in order to study the accuracy of the parameters obtained. Variations of ±5 to 7% of the Debye–Waller factors were observed, while the scale factor varied only within 1%. These variations show the inaccuracy of the B values due to random errors in the large-angle reflections. No particular trend could be observed in the dependence of

the B values on the cut-off, but the variations seem to be random oscillations around constant average values given in Table 2. Consequently the data do not indicate deviations of the ionic form factors from the theoretical ones beyond sin $\theta/\lambda = 0\cdot5$ Å^{-1}. This does not, however, mean experimental confirmation of the theoretical atomic factors, but that in the region from about 0·5 Å^{-1} to the experimental limit of sin θ/λ the adjustment of the Debye–Waller factors and the scale parameter is able to fit the theoretical behaviour to the experimental one. In any case, all obtainable information on bonding or atomic deformations is included in the structure factors at smaller scattering angles.

For MgO the data of Sanger (1969) were introduced because of the comparable experimental technique.

After the preliminary treatment the experimental structure factors F_0 are on an absolute scale and corrected for anomalous dispersion and for thermal diffuse scattering. The F_0 form the starting values of the charge density analysis. In the final analysis the low-scattering-angle data of Table 3 were used. All experi-mental information given by the higher-order data is

Table 3. *Theoretical (F_c) and experimental (F_0) structure amplitudes and experimental errors δF used in the analysis*

		MgO (Sanger, 1969)			CaO		
h k l	b = 2 sinθ/λ	F_c	F_0	b	F_c	F_0	δF
1 1 1	0.411	11.565	11.413	0.359	34.02	33.35	0.40
2 0 0	0.474	52.770	54.181	0.415	78.47	77.44	0.77
2 2 0	0.671	41.002	41.029	0.587	61.99	60.48	0.50
3 1 1	0.787	12.804	12.264	0.688	27.92	25.75	0.31
2 2 2	0.822	33.806	32.956	0.719	52.14	52.43	0.53
4 0 0	0.949	28.804	29.067	0.830	45.69	44.95	0.45
3 3 1	1.034	9.792	9.484	0.904	23.59	23.30	0.43
4 2 0	1.061	25.089	24.145	0.928	41.20	41.18	0.55
4 2 2	1.162	22.216	22.145	1.017	37.90	36.74	0.37
5 1 1	1.233	7.219	7.076	1.078	20.99	20.55	0.36
3 3 3	1.233	7.219	7.337	1.078	20.99	20.48	0.27
4 4 0	1.342	18.067	17.918	1.174	33.31	32.53	0.36
5 3 1	1.404	5.318	5.261	1.228	19.18	19.53	0.08
4 4 2	1.424	16.523	16.674	1.245	31.60	32.06	0.26
6 0 0	1.424	16.523	16.554	1.245	31.60	31.41	0.15
6 2 0	1.500	15.221	15.360				
5 3 3	1.556	3.955	3.978				
6 2 2	1.574	14.109	14.066				
4 4 4	1.644	13.147	13.235				
7 1 1	1.694	2.983	3.159				
5 5 1	1.694	2.983	3.159				

	SrO				BaO			
h k l	b	F_c	F_0	δF	b	F_c	F_0	δF
1 1 1	0.335	99.2	99.8	1.0	0.313	159.5	155.7	2.2
2 0 0	0.386	142.2	144.8	1.2	0.361	203.7	201.6	2.6
2 2 0	0.546	119.7	120.2	1.4	0.511	173.9	172.5	2.1
3 1 1	0.641	83.8	83.8	1.5	0.599	129.3	126.2	1.8
2 2 2	0.669	105.2	106.1	1.2	0.625	154.0	156.8	1.9
4 0 0	0.773	95.0	96.0	0.8	0.722	139.4	141.6	1.7
3 3 1	0.842	73.4	76.7	1.5	0.787	110.7	108.3	2.2
4 2 0	0.864	87.2	87.7	0.9	0.807	127.8	130.2	2.0
4 2 2	0.946	80.9	80.7	0.9	0.884	118.2	114.4	1.9
3 3 3					0.938	96.9	100.2	1.8
5 1 1					0.938	96.9	95.3	1.3

Table 2. *Fourier-refined Debye–Waller factors*

	MgO	CaO	SrO	BaO
B_+ (Å^2)	0·420	0·35 ± 0·01	0·43 ± 0·02	0·79 ± 0·02
B_- (Å^2)	0·343	0·44 ± 0·01	1·93 ± 0·06	1·19 ± 0·03

included in the obtained values of the Debye–Waller factors. Their inclusion in the further analysis would only cause disturbing variations in the experimental charge densities due to the same statistical errors which made the B values vary as a function of the cut-off.

The uncertainties δF are the standard errors (of the mean) for each group of three experimental determinations. Thus, they give estimates of random errors but do not attempt to include systematic errors.

Spherical behaviour of the atoms

To discuss the ionic state of the atoms and their bonding we calculated the radial charge densities $4\pi r^2 \rho_0(r)$, where

$$\rho_0(r) = \frac{1}{V} \sum_j F_j \frac{\sin 2\pi b_j r}{2\pi b_j r} \qquad (1)$$

and the spherical electron counts

$$Z_0(r) = \int_0^r 4\pi r^2 \rho_0 \, dr = \frac{4\pi r^3}{V} \sum_j F_j \frac{j_1(2\pi b_j r)}{2\pi b_j r} \qquad (2)$$

for each ion. The residual terms of the series were taken into account by calculating these quantities for a crystal with Gaussian atoms showing accurate fit to the theoretical atomic factors beyond the experimental cut-off value of $\sin \theta / \lambda$, and by adding to these results the respective difference series (1) and (2).

The results are shown in Figs. 1 to 8. They show each ion to be separated from its surroundings by a distinct minimum in the radial density, followed by a steep rise due to the nearest neighbours. The structure can, thus, be described as a dense packing of over-
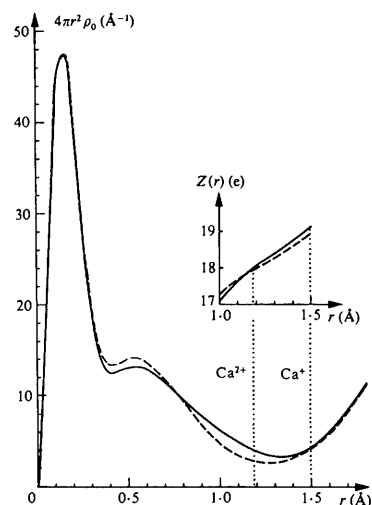

Fig. 2. Radial charge density and electron counts around Ca^{2+} in CaO. Experimental curves (———), theoretical curves (– – –).
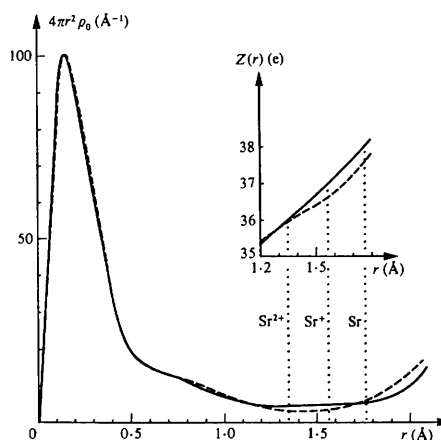

Fig. 3. Radial charge density and electron counts around Sr^{2+} in SrO. Experimental curves (———), theoretical curves (– – –).

Fig. 1. Radial charge density and electron counts around Mg^{2+} in MgO. Experimental curves (———), theoretical curves (– – –).
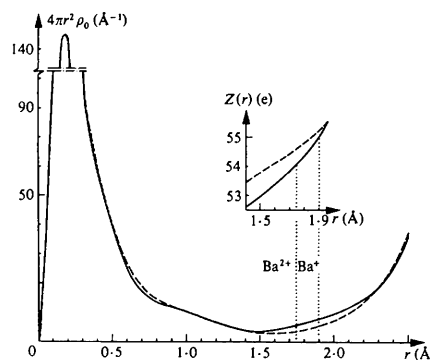

Fig. 4. Radial charge density and electron counts around Ba^{2+} in BaO. Experimental curves (———), theoretical curves (– – –).

Table 4. *Characteristics of the radial densities: R = radius of best separation, $4\pi R^2 \rho_0(R)$ = minimum of the radial density, $Z_0(R)$ and $Z_4(R)$ = electron count and charge transfer of the K_4 type deformation, respectively, within the radius R*

| | R (Å) | | $4\pi R^2 \rho_0(R)$ (e Å^{-1}) | | $Z_0(R)$ | | $Z_4(R)$ |
	Theor.	Exp.	Theor.	Exp.	Theor.	Exp.	Exp.
Cation:							
Mg	0·92	1·03	1·88	2·3	10·16	10·64	0·04
Ca	1·28	1·32	2·62	3·1 ± 0·5	18·30	18·5 ± 0·15	−0·12 ± 0·09
Sr	1·42	1·27	3·04	4·2 ± 1·3	36·2	35·7 ± 0·35	−0·22 ± 0·17
Ba	1·61	1·49	3·12	3·7 ± 2·1	54·1	52·7 ± 0·7	0·15 ± 0·4
Oxygen in:							
MgO	1·28	1·28	3·45	2·8	9·05	9·14	0·17
CaO	1·31	1·19	3·14	2·3 ± 0·5	9·05	8·4 ± 0·15	0·10 ± 0·07
SrO	1·36	1·44	3·21	1·2 ± 1·3	9·13	9·5 ± 0·4	0·46 ± 0·22
BaO	1·45	1·24	3·17	1·2 ± 1·5	9·47	8·8 ± 0·6	0·45 ± 0·25

lapping ions. This behaviour is similar to that observed in several ionic crystals and metal oxides, *cf.* Kurki-Suonio & Salmo (1971), Ruuskanen & Kurki-Suonio (1973), Vahvaselkä & Kurki-Suonio (1975), and

different from that observed in the presence of local bonds, *cf.* Kurki-Suonio & Ruuskanen (1971), or metallic bonding, *cf.* Pesonen (1974), Rantavuori (1977).
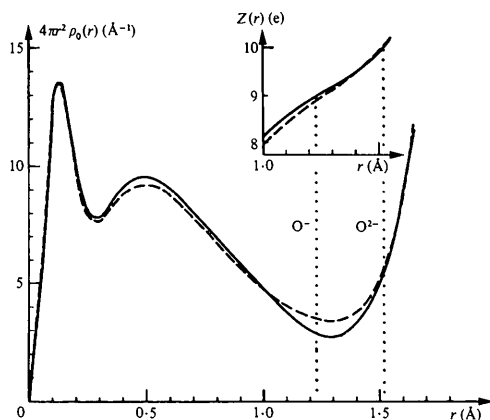

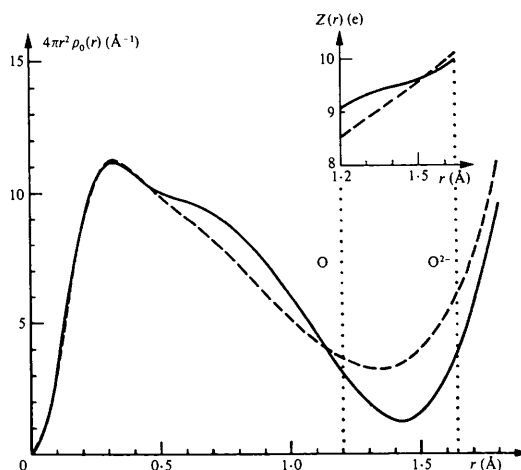Fig. 5. Radial charge density and electron counts around O^{2-} in MgO. Experimental curves (———), theoretical curves (———).
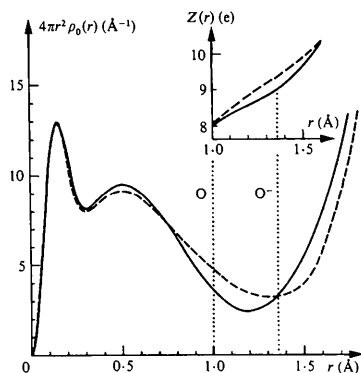

Fig. 6. Radial charge density and electron counts around O^{2-} in CaO. Experimental curves (———), theoretical curves (———).

Fig. 7. Radial charge density and electron counts around O^{2-} in SrO. Experimental curves (———), theoretical curves (———).
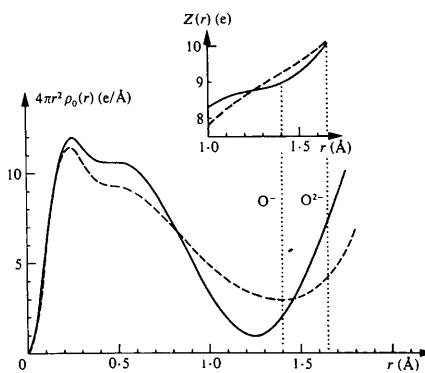

Fig. 8. Radial charge density and electron counts around O^{2-} in BaO. Experimental curves (———), theoretical curves (———).

Table 4 lists some numerical characteristics of the spherical behaviour. The distance of the minimum in the radial density is the radius of the best overall separation of the atom from its surroundings. The value of the radial density at the minimum shows the degree of this separability and is a measure of the conceptual uncertainty of the experimental 'atom'. The electron count within this radius gives the total electronic charge concentrated locally at the atom and gives, thus, a basis for discussing the ionic state of the atom.

The error limits given in Table 4 refer to the statistical errors of the quantities at the fixed value R of the radius. They show, thus, the magnitude of the error bars which should be attached to the experimental curves. So, for $Z_0(R)$ they do not indicate the accuracy of the values as experimental estimates of the ionic state of the atoms. A major part of the inaccuracy of such an interpretation obviously comes from the conceptual indeterminacy due to overlapping or, rather, inseparability of the ions. The statistical error limits are not given for MgO since the standard deviations of the experimental structure factors were not known.

As compared to the atomic superposition model, represented by the theoretical curves in Figs. 1 to 8, several systematic features can be noted. The oxygen atom is compressed, yielding a lower minimum value of radial density and, hence, less overlapping with neighbours. This effect, which tends to make oxygen a better defined entity, gets stronger with increasing atomic number of the cation. The cations correspondingly show a slight extension, though for the heavy Sr and Ba ions this statement is not significant. This behaviour indicates dominance of ionic nature of the bonding and increase of ionicity with increasing atomic number of the cation.

This is confirmed by the electron counts, though the uncertainties in the cases of SrO and BaO are rather large. In MgO, the electron counts are close to the situation Mg^+O^- and practically all electrons are concentrated in the counted volumes of the peaks. The number of electrons outside the counted regions seems to increase with increasing atomic number of the cation. For the other compounds the results rather refer to the state $X^{2+}O^{2-}$ with the tenth electron of O^{2-} distributed widely in the surroundings, although for SrO and BaO the accuracy is not sufficient for conclusive statements.

Non-spherical analysis

Next, the radial scattering factors $f_n(b)$ in the cubic harmonic expansion

$$f(\mathbf{b}) = \sum f_n(b) K_n(\theta_b, \varphi_b)$$

of the atomic factor of each ion were calculated from the series,

$$f_n(b,R) =$$

$$\frac{(4\pi)^2 R^3}{VA_n} \sum_j F_j K_n(\theta_j, \varphi_j) \frac{x j_{n+1}(x) j_n(x_j) - x_j j_{n+1}(x_j) j_n(x)}{x^2 - x_j^2}$$

with $x = 2\pi Rb$ (Kurki-Suonio, 1967).

The computational atomic radii R were taken slightly larger than the radii of best separation of Table 4 (Kurki-Suonio, 1968).

The calculation was done up to the tenth order and the difference series results are shown in Figs. 9 to 16 for all orders yielding observable values in the scale of the figures. The error bars give the statistical accuracy corresponding to the δF values of Table 3.

The spherical components Δf_0 are equivalent to the differences of the experimental and theoretical curves in Figs. 1 to 8. With their error bars they show the significance of the statements concerning electron transfer, compression or extension of the ions in the integrated sense.
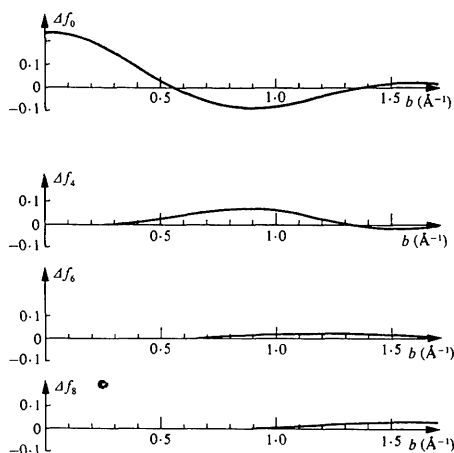

Fig. 9. Radial atomic factors Δf_n of Mg^{2+} in MgO within the radius $r = 1.15$ Å.
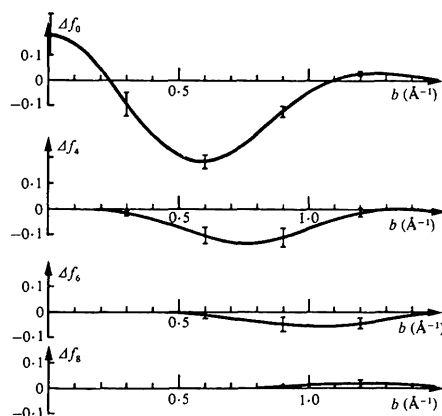

Fig. 10. Radial atomic factors Δf_n of Ca^{2+} in CaO within the radius $r = 1.40$ Å.

The nonsphericities are expected to be of low-order harmonic nature. In this case only the fourth order is expected to be of physical origin. It shows the strength of a cubic K_4-type deformation, which involves charge transfer from [111] to [100] or the nearest-neighbour directions. The numbers Z_4 in Table 4 give, within the radius of best separation, the electron counts under the positive lobes of $K_4(\theta,\varphi)$ in the hexadecapole terms

$\rho_4(r)K_4(\theta,\varphi)$ of the ionic charge distributions, cf. Kurki-Suonio (1977). Thus, they represent the total amount of charge transferred to produce the fourth-order deformation.

The magnitudes of the higher-order components give a measure of the inconsistency of the nonspherical information included in the data (Kurki-Suonio & Ruuskanen, 1971), and will in this context allow no physical interpretation.

Oxygen is deformed in all four crystals, in CaO less than in MgO, and very strongly in SrO and BaO. The deformation is positive, i.e. gives an excess of charge in the nearest-neighbour directions. The deformations of the cations are much smaller. Mg and Ba show no detectable nonsphericity. In Ca and Sr the deformation
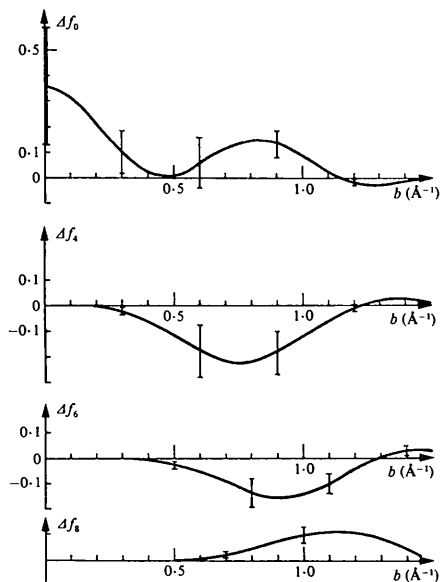
Fig. 11. Radial atomic factors Δf_n of Sr^{2+} in SrO within the radius $r = 1.55$ Å.

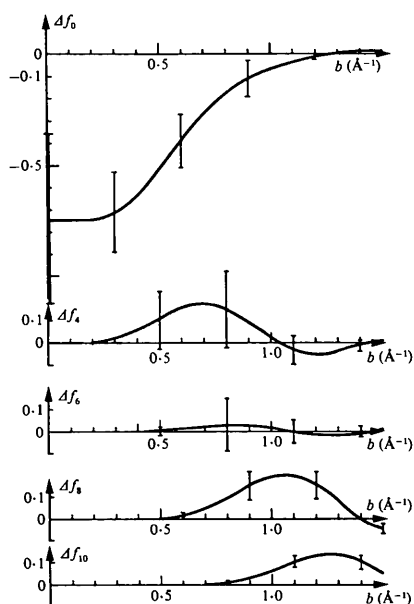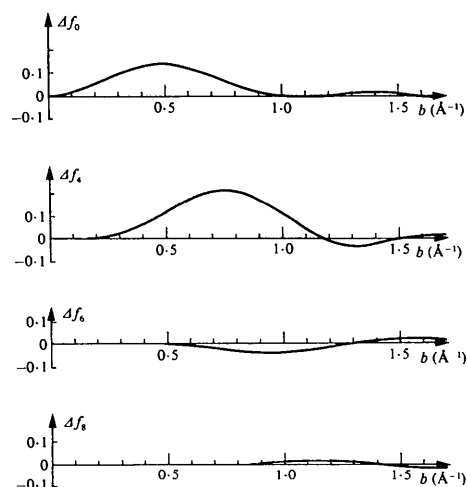Fig. 13. Radial atomic factors Δf_n of O^{2-} in MgO within the radius $r = 1.40$ Å.

Fig. 12. Radial atomic factors Δf_n of Ba^{2+} in BaO within the radius $r = 1.65$ Å.

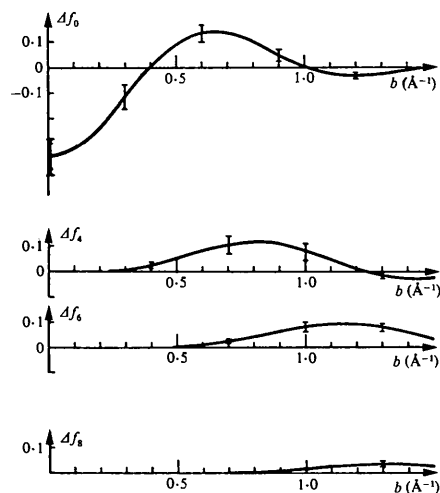Fig. 14. Radial atomic factors Δf_n of O^{2-} in CaO within the radius $r = 1.30$ Å.

is negative, indicating charge transfer from [100] to the [111] direction, but the significance of the results is questionable.

Discussion

Factors affecting the reliability of the results obtained in the analysis are divided conventionally into three groups:

1. Random errors of experimental structure factors;
2. Errors due to experimental cut-off in sin θ/λ;
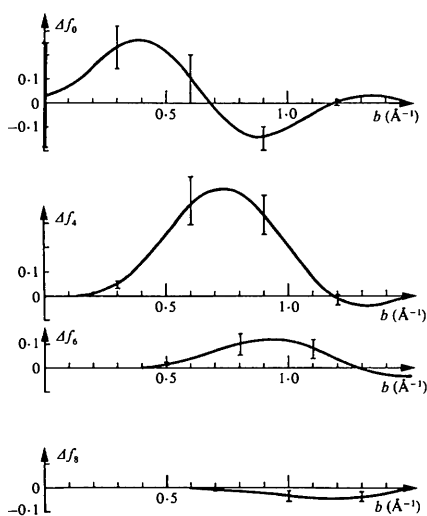3. Systematic sources of error.

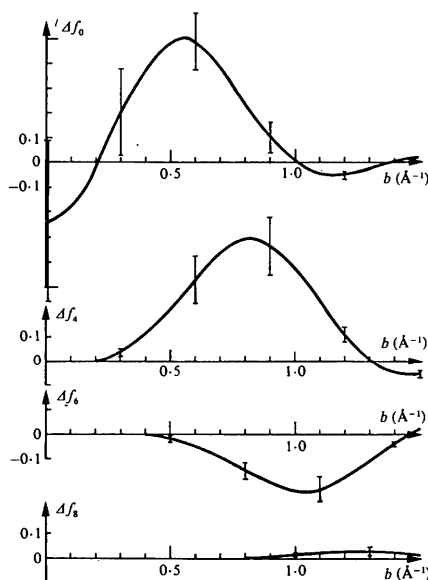Fig. 15. Radial atomic factors Δf_n of O^{2-} in SrO within the radius $r = 1.50$ Å.

Fig. 16. Radial atomic factors Δf_n of O^{2-} in BaO within the radius $r = 1.35$ Å.

The error bars and error limits given in the figures and tables show the statistical significance of the results with respect to random errors.

In real-space calculations of the spherical analysis the cut-off errors have been eliminated by the Gaussian method. Accuracy of the residual-term calculation is an order of magnitude better than the statistical accuracy, except for the very central region of atoms (Hosemann & Bagchi, 1962; Vahvaselkä & Kurki-Suonio, 1975). As a further check, calculations were done using different theoretical atomic factors and even atoms in different states of ionization as the basis of the Gaussian calculation. These checks involved, for instance, the superpositions $Ca^{2+}O$, BaO and $Ba^{2+}O^{2-}$ with scattering factors of Doyle & Turner (1968) and Cromer & Mann (1968). The Debye–Waller factors varied slightly, 2 and 3% for CaO and BaO respectively, but the resulting experimental radial densities did not differ in the scale of the figures, showing that the residual terms of different models are essentially equal.

In the reciprocal-space calculations of the non-spherical analysis the cut-off errors are significant only near the cut-off value of sin θ/λ (Kurki-Suonio, 1968). Thus, the cut-off errors do not affect our conclusions.

The effects of systematic experimental errors are most difficult to judge.

As a result of the growth by arc fusion, lattice imperfections were already present. This effect was strengthened by the extreme vulnerability of the crystals. On the other hand, the experimental arrangements necessary to protect the samples limited the experimental accuracy. All these experimental difficulties gave rise to absorption-correction uncertainties, emphasized further by the high absorption coefficients (Table 1).

The values obtained for the Debye–Waller factors should be compared with the mean square amplitudes obtained from lattice-dynamical calculations (Galtier & Montaner, 1975). For MgO, other experimental determinations can be compared (Lawrence, 1973; Togawa, 1965). Although the present measurement is not particularly suited for conclusions on these quantities, some of the discrepancies are too large to be explained by the experimental inaccuracies in this study. Both the theoretical and the experimental values for O in SrO are obviously anomalous; the former is small and the latter very large, beyond explanation as an experimental error. The study of different crystals cut from the same large crystal of SrO always indicated this anomaly. Lattice defects may offer a partial interpretation of it.

Variations in the radial densities, as well as the changes of the obtained B values with the cut-off, indicated that there were some errors present in the high-order data, larger than those estimated from experimental conditions. The reduced data sets used in the final analysis show, however, no obvious inconsistencies, neither as variations of radial density nor as

the occurrence of large high-order non-sphericities. This gives indirect evidence in favour of the results of the charge-density analysis, independently of the reliability of the Debye–Waller factors. The systematic nature of the results is another supporting argument.

The results are in qualitative agreement with some other considerations of these crystals. The increasing ionicity with increasing atomic number of the cation is noticed in the measurements of elastic constants by Son & Bartels (1972) and by Bartels & Vetter (1973) and in infrared spectroscopy by Galtier (1973) and Montaner (1974). It might be possible to relate the slightly stronger deformation of oxygen together with the lack of negative deformation of the cation in MgO, as compared to CaO, to the occurrence of covalency. This would agree with the successful treatment of covalent effects in MgO by Gillis (1971) in connection with lattice-dynamical calculations.

In the case of MgO this work gives another example that direct counting of electrons may give results essentially different from those concluded from a comparison of structure factors, cf. Kurki-Suonio & Salmo (1971) and Sanger (1969). Representation of oxygen as a doubly ionized local entity in these crystals is not satisfactory. A total of about one electron, the tenth electron of O^{2-}, is widely distributed in the interatomic space, or partly caught by the other ion as in MgO, and will therefore have a behaviour quite different from the main part of the ion, for example, in dynamical contexts. The results of Göttlicher & Kieselbach (1976) on LiOH indicate similar behaviour giving 8·7 electrons localized inside a sphere around the oxygen atom.

The contributions of Hannu Kurki-Suonio, Matti Merisalo, Riitta Sälke and Aino Vahvaselkä to programming and computation are gratefully acknowledged.

References

BARTELS, R. A. & VETTER, V. H. (1972). *J. Phys. Chem. Solids*, **33**, 1991–1992.
BURLEY, G. (1965). *J. Phys. Chem. Solids*, **26**, 1605–1613.
BUSING, W. R. & LEVY, H. A. (1957). *Acta Cryst.* **10**, 180–187.
CHEN, Y. & ABRAHAM, M. (1972). *2nd National Conference on Crystal Growth*, p. 15. American Association for Crystal Growth.
COOPER, M. J. & ROUSE, K. D. (1968). *Acta Cryst.* A**24**, 405–410.
COPPENS, P. & HAMILTON, W. C. (1970). *Acta Cryst.* A**26**, 71–83.

CROMER, D. T. & LIBERMAN, D. (1970). *J. Chem. Phys.* **53**, 1891–1898.
CROMER, D. T. & MANN, J. B. (1968). *Acta Cryst.* A**24**, 321–324.
DAWSON, B. (1969). *Acta Cryst.* A**25**, 12–2ą.
DENNE, W. A. (1972). *Acta Cryst.* A**28**, 192–201.
DOYLE, P. A. & TURNER, P. S. (1968). *Acta Cryst.* A**24**, 390–397.
GALTIER, M. (1973). Thesis, CNRS, AO No. 9118.
GALTIER, M. & MONTANER, A. (1975). *Phys. Status Solidi*, **70**, 163–172.
GILLIS, N. S. (1971). *Phys. Rev.* B**3**, 1482–1496.
GÖTTLICHER, S. & KIESELBACH, B. (1976). *Acta Cryst.* A**32**, 185–192.
HOSEMANN, R. & BAGCHI, S. N. (1962). *Direct Analysis of Diffraction by Matter*. Amsterdam: North-Holland.
International Tables for X-ray Crystallography (1974). Vol. IV. Birmingham: Kynoch Press.
KURKI-SUONIO, K. (1967). *Ann. Acad. Sci. Fenn.* AVI, No. 263.
KURKI-SUONIO, K. (1968). *Acta Cryst.* A**24**, 379–390.
KURKI-SUONIO, K. (1977). *Isr. J. Chem.* **16**, 115–123.
KURKI-SUONIO, K. & RUUSKANEN, A. (1971). *Ann. Acad. Sci. Fenn.* AVI, No. 358.
KURKI-SUONIO, K. & SALMO, P. (1971). *Ann. Acad. Sci. Fenn.* AVI, No. 369.
LAWRENCE, J. L. (1973). *Acta Cryst.* A**29**, 94–95.
MILLEDGE, H. J. (1969). *Acta Cryst.* A**25**, 173–180.
MONTANER, A. (1974). Thesis, CNRS AO No. 9448.
PAAKKARI, T. (1975). Private communication.
PESONEN, A. (1974). *Phys. Fenn.* **9**, 121–128.
PHILLIPS, J. C. (1970). *Rev. Mod. Phys.* **42**, 317–356.
RACCAH, P. M. & ARNOTT, R. J. (1967). *Phys. Rev.* **153**, 1028–1031.
RANTAVUORI, E. (1977). Thesis, Laboratory of Physics, Helsinki Univ. of Technology, Res. Rep. 6/1977.
RIEDER, K. H., WEINSTEIN, A., CARDONA, M. & BILZ, H. (1973). *Phys. Rev.* B**8**, 4780–4786.
RUUSKANEN, A. & KURKI-SUONIO, K. (1973). *J. Phys. Soc. Jpn*, **34**, 715–719.
SANGER, P. L. (1969). *Acta Cryst.* A**25**, 694–702.
SON, P. R. & BARTELS, R. A. (1972). *J. Phys. Chem. Solids*, **33**, 819–825.
SUZUKI, T. (1960). *Acta Cryst.* **13**, 279.
TOGAWA, S. (1965). *J. Phys. Soc. Jpn*, **20**, 742–752.
TOGAWA, S., INKINEN, O. & MANNINEN, S. (1971). *J. Phys. Soc. Jpn*, **30**, 1132–1135.
TOKONAMI, H. (1965). *Acta Cryst.* **19**, 486.
VAHVASELKÄ, A. & KURKI-SUONIO, K. (1975). *Phys. Fenn.* **10**, 87–99.
VETTER, V. H. & BARTELS, R. A. (1973). *J. Phys. Chem. Solids*, **34**, 1448–1449.
WATSON, R. E. (1958). *Phys. Rev.* **111**, 1108–1110.
WEISS, R. J. (1970). *Philos. Mag.* **21**, 1169–1173.
YAMASHITA, J. & ASANO, S. (1970). *J. Phys. Soc. Jpn*, **28**, 1143–1150.
YAMASHITA, J. & KOJIMA, M. (1952). *J. Phys. Soc. Jpn*, **7**, 261–263.